

Stimulated Raman spin-coherence and spin-flip induced hole burning in charged GaAs quantum dots

Jun Cheng,^{1,*} Wang Yao,^{2,†} Xiaodong Xu,¹ D. G. Steel,^{1,‡} A. S. Bracker,³ D. Gammon,³ and L. J. Sham²

¹*The H. M. Randall Laboratory of Physics, The University of Michigan, Ann Arbor, MI 48109*

²*Department of Physics, The University of California-San Diego, La Jolla, CA 92093*

³*The Naval Research Laboratory, Washington D. C. 20375*

High-resolution spectral hole burning (SHB) in coherent non-degenerate differential transmission spectroscopy discloses spin-trion dynamics in an ensemble of negatively charged quantum dots. In the Voigt geometry, stimulated Raman spin coherence gives rise to Stokes and anti-Stokes sidebands on top of the trion spectral hole. The prominent feature of an extremely narrow spike at zero detuning arises from spin population pulsation dynamics. These SHB features confirm coherent electron spin dynamics in charged dots and the linewidths reveal spin spectral diffusion processes.

PACS numbers: 71.35.Pq, 42.65.-k, 78.67.Hc

Single electron spin localized in semiconductor quantum dots (QDs) has attracted a great deal of interest due to its potential use in quantum applications [1]. Experimental and theoretical efforts have been focused on controllable coherent spin dynamics and possible decoherence mechanisms [2, 3, 4, 5, 6, 7, 8, 9, 10, 11, 12, 13, 14]. In this paper, we report spectral hole burning (SHB) in coherent differential transmission (DT) spectroscopy induced by spin-trion dynamics in an ensemble of negatively charged QDs. Spin coherence induced SHB by stimulated Raman excitation and spin relaxation induced SHB due to the population pulsation dynamics are observed in the QD system. Features of SHB not only disclose important spin dynamics observed from transient spectroscopy [2] and phase modulation techniques [11], but also provide information on spin spectral diffusion (SD) processes [14] which are not easily revealed by previous methods.

The interface fluctuation GaAs/Al_{0.3}Ga_{0.7}As QDs are molecular beam epitaxy grown with growth interrupts, and modulation Si doping in the barrier incorporates excess electrons [15]. The pump $E_1(\omega_1)$ and probe $E_2(\omega_2)$ optical fields are derived from two frequency-stabilized and independently tunable CW lasers with a mutual coherence bandwidth of 20 neV, which is crucial for this experiment as discussed below. The sample is kept inside a superconducting magnetic liquid helium flow cryostat and the temperature is maintained at 4.5 K. The DT signal is homodyne detected with the probe field by a photodiode and extracted by a lock-in amplifier.

A nonlinear degenerate DT spectrum with $\omega_1 = \omega_2$ [Fig. 1(a)] shows the trion and exciton ensemble resonances. Their assignments are confirmed by both photoluminescence and transient quantum beats studies (data not shown). The trion binding energy (i.e., the separation between exciton and trion resonances) is measured to be 2.9 meV, in agreement with earlier reports of photoluminescence [15] and transient spectroscopy [2]. The ensemble trion inhomogeneous broadening width (~ 2.5 meV) can be estimated from the broad Gaussian profile

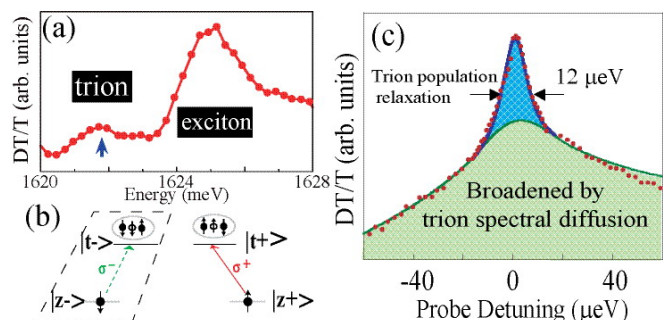


FIG. 1: (a). Coherent degenerate DT spectrum of both trion and exciton ensemble resonances. The arrow shows the fixed pumping position for (c). (b). Energy level diagram of charged QDs in absence of magnetic field, where solid (empty) circles indicate electrons (holes) and arrows show the corresponding spin orientations. The single electron ground state has either spin down ($|z-\rangle$) or spin up ($|z+\rangle$). The trion state consists of two-electron singlet state and one heavy hole with spin down ($|t-\rangle$) or spin up ($|t+\rangle$). σ^- (σ^+) light couples $|z-\rangle$ ($|z+\rangle$) to $|t-\rangle$ ($|t+\rangle$). (c) A clear view of the trion spectral hole burning profile, shown as a double Lorentzian, where the probe is detuned relative to pump position (1621.9 meV).

of the trion resonance.

To study SHB with non-degenerate DT spectroscopy, the pump beam is fixed near the trion ensemble peak and the probe beam is detuned ($\Delta \equiv \omega_2 - \omega_1$). A narrow spectral structure appears, exhibiting a double-Lorentzian-like shape, i.e., a narrower Lorentzian peak on top of a broader one [Fig. 1(c)]. As established below, the narrower Lorentzian peak is due to the trion population relaxation dynamics and its linewidth ($\sim 12 \mu\text{eV}$) gives the trion population relaxation rate. The broader Lorentzian peak ($\sim 50 \mu\text{eV}$) underneath this resonance is due to trion population relaxation and coherence decay broadened by the trion SD process. This complex lineshape and its unfolded SHB features with a magnetic field in the Voigt geometry are the focus of our study.

The dynamics of the QD ensemble in the presence of

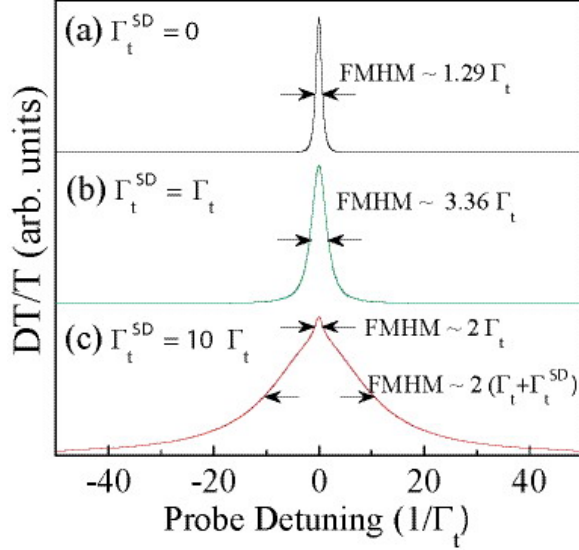


FIG. 2: The calculated SHB lineshape of 2-level system with different spectral diffusion rates, where $\Lambda_t = 1000\Gamma_t$ and $\gamma_t = \Gamma_t/2$. (a). $\Gamma_t^{SD} = 0$. (b). $\Gamma_t^{SD} = \Gamma_t$. (c). $\Gamma_t^{SD} = 10\Gamma_t$.

the radiation field and various interactions with the environment is described by the modified optical Bloch equation (OBE) [16]:

$$i\hbar\dot{\rho}(\epsilon) = [H, \rho(\epsilon)] + \left. \frac{\partial \rho(\epsilon)}{\partial t} \right|_{\text{relax}} + \left. \frac{\partial \rho(\epsilon)}{\partial t} \right|_{\text{SD}} \quad (1)$$

where $\rho(\epsilon)$ is the density matrix of each ensemble member

characterized by its resonance energy ϵ . H is the total Hamiltonian including the interaction with the coherent optical fields. The second term on the RHS is a generalized relaxation term that describes population decay and pure dephasing. The last term is due to various SD processes [17]. Eq. (1) without the SD term reduces to the standard OBE.

Considering the optical selection rules in the absence of a magnetic field, the transition from spin ground state $|z-\rangle$ ($|z+\rangle$) to trion state $|t+\rangle$ ($|t-\rangle$) is forbidden as a dark transition [15]. Therefore, with co-circularly polarized pump and probe fields, the charged QD energy levels reduce to a 2-level system, as shown in the enclosed box in Fig. 1(b). The relevant SD process here is the interdot transfer of trion population [18]

$$\begin{aligned} \left. \frac{\partial \rho_{\bar{t}, \bar{t}}(\epsilon)}{\partial t} \right|_{\text{SD}} &= -\Gamma_t^{SD}(\epsilon) \rho_{\bar{t}, \bar{t}}(\epsilon) + \int W_t(\epsilon, \epsilon') \rho_{\bar{t}, \bar{t}}(\epsilon') d\epsilon', \\ \left. \frac{\partial \rho_{\bar{t}, \bar{z}}(\epsilon)}{\partial t} \right|_{\text{SD}} &= -\Gamma_t^{SD}(\epsilon) \rho_{\bar{t}, \bar{z}}(\epsilon). \end{aligned} \quad (2)$$

where $W_t(\epsilon, \epsilon')$ is the spectral redistribution kernel representing the rate for trion population to migrate from a dot with resonant energy ϵ' to dots with energy ϵ . While this interdot transfer conserves the ensemble trion population, the dipole coherence is lost. $\Gamma_t^{SD}(\epsilon) = \int W_t(\epsilon', \epsilon) d\epsilon'$ is the overall SD rate. For an optically thin sample, the DT spectrum is given by the imaginary part of the third order induced optical polarization integrated over the inhomogeneous distribution [19, 20],

$$\begin{aligned} P_{\text{NL}}^{(3)} \simeq & -\frac{iN|\mu|^4|E_1|^2E_2^*}{2\hbar^3\Lambda_t} \left\{ \frac{1}{\Gamma_t + \Gamma_t^{SD} + i\Delta} \left[\frac{1}{\Lambda_t} + \frac{\sqrt{\pi}}{2(\gamma_t + \Gamma_t^{SD}) + i\Delta} \right] + \frac{\pi}{\Gamma_t\Lambda_t} \frac{\Gamma_t^{SD}}{\Gamma_t + \Gamma_t^{SD}} \right. \\ & \left. + \frac{\sqrt{\pi}}{\Gamma_t + \Gamma_t^{SD}} \frac{1}{2(\gamma_t + \Gamma_t^{SD}) + i\Delta} + \frac{\pi}{\Lambda_t(\Gamma_t + i\Delta)} \frac{\Gamma_t^{SD}}{\Gamma_t + \Gamma_t^{SD} + i\Delta} \right\} \end{aligned} \quad (3)$$

where Γ_t (γ_t) is trion population (coherence) decay rate, N is the total number of excited charged QDs, Λ_t is the ensemble inhomogeneous broadening width of the trion resonance and μ the optical dipole of a single dot. We have assumed a redistribution kernel $W_t(\epsilon, \epsilon') = \Gamma_t^{SD} \exp(-(\epsilon - \bar{\epsilon})^2/(\Lambda_t^2))/(\sqrt{\pi}\Lambda_t)$ where $\bar{\epsilon}$ is the ensemble averaged resonance energy [21]. Eq. (3) holds when the approximation of plasma dispersion function is taken [22] because $\Gamma_t, \gamma_t, \Gamma_t^{SD}, \Delta \ll \Lambda_t$ and the pump frequency is fixed near the center of the ensemble trion spectrum.

The SD process significantly changes the trion SHB lineshape and linewidth, which can be discussed in three regimes, as schematically shown in Fig. 2. $\Gamma_t = 2\gamma_t$ is

assumed only for the theoretical calculation in Fig. 2 to simplify discussions, since pure dephasing has been found negligible for trion states at 4.5 K [23]. When $\Gamma_t^{SD} \ll \Gamma_t$, the trion SHB in the DT spectrum reduces to the standard Lorentzian squared with width $\sim \Gamma_t$. Secondly, when $\Gamma_t^{SD} \simeq \Gamma_t$, the trion SHB lineshape is $(24\Gamma_t^2 + \Delta^2)[(\Gamma_t + \Gamma_t^{SD})^2 + \Delta^2]^{-1}[(\Gamma_t + 2\Gamma_t^{SD})^2 + \Delta^2]^{-1}$ where the linewidth is considerably broadened by the SD process. Finally, when $\Gamma_t^{SD} \gg \Gamma_t$, the lineshape changes to a double Lorentzian-like profile with larger FWHM of $2(\Gamma_t + \Gamma_t^{SD})$ and smaller FWHM of $2\Gamma_t$. The physical origin of the narrower Lorentzian is due to the population pulsation effect [24]. This explains the observed lineshape

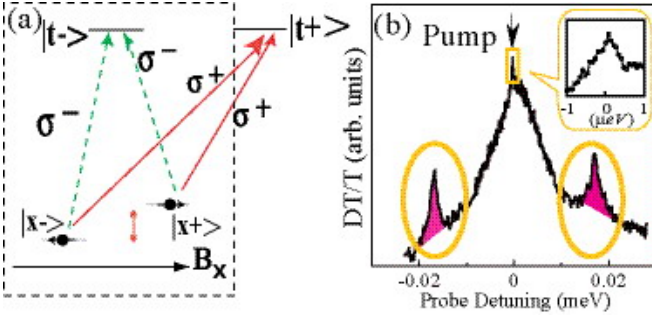


FIG. 3: (a). Energy level scheme of charged dot in Voigt geometry ($B_x \neq 0$). The new ground states $|x\pm\rangle$ denote electron spin orientation along the x -axis separated by Zeeman splitting. The new selection rules are labelled by solid (dashed) lines with σ^+ (σ^-) light. (b). The newly-emerged center sharp spike and two symmetric sidebands at $B_x = 2.2$ T, where the fixed pump is indicated by the arrow. The two Stokes and anti-Stokes spin-coherence induced sidebands are highlighted. The inset shows the zoomed in sharp central spike at $\Delta \sim 0$. A similar figure was first presented in Ref. [11] but with a different objective.

shown in Fig. 1(c), which is consistent with the physical model (Eq. (3)) assuming $\hbar\Gamma_t \simeq 7\mu\text{eV}$, $\hbar\gamma_t \simeq 8\mu\text{eV}$, $\hbar\Gamma_t^{SD} \simeq 46\mu\text{eV}$, and $\hbar\Lambda_t \simeq 1000\mu\text{eV}$ plus a slow linear slope. The values of Γ_t and γ_t agree with earlier reports [2, 23] and the value of Λ_t is in agreement with the degenerate DT trion ensemble resonance in Fig. 1(a). The relatively big Γ_t^{SD} implies trion SD process plays an important role.

With a magnetic field applied perpendicular to QD growth direction (i.e., Voigt geometry), the spin eigenstates $|x\pm\rangle$ along the field direction are split in energy due to the non-zero electron in-plane g -factor (g_x^e) while the trion states are unaffected as the heavy-hole in-plane g -factor is negligible [25]. The new eigenstates and optical selection rules are shown in Fig. 3(a) [2]. With co-circularly polarized pump and probe fields, the relevant states form a three-level Λ -system enclosed in the dashed box. Utilizing a similar Λ -system, optical pumping leading to spin cooling has been reported recently in different structural QDs [26, 27]. However, no similar optical pumping effect was observed in our system, where the strong spectral diffusion on two spin ground states discussed below plays an important role.

The SHB profile changes dramatically in this Voigt geometry. An ultra-sharp central spike appears on top of the trion spectral hole, as highlighted by the square region in Fig. 3(b). The physical origin can be understood from analysis of the perturbation pathway:

$$\rho_{\bar{x},\bar{x}}^{(0)} \xrightarrow{E_1^*} \rho_{\bar{x},\bar{x}}^{(1)} \xrightarrow{E_2} \rho_{\bar{x},\bar{x}}^{(2)} \xrightarrow{\Gamma_t} \rho_{\bar{x},\bar{x}}^{(2)} \xrightarrow{E_1} \rho_{\bar{x},\bar{x}}^{(3)} \quad (4)$$

The pump field E_1^* and probe field E_2 create a second order spin population $\rho_{\bar{x},\bar{x}}^{(2)}$ through the population decay of the trion, which oscillates at the detuning frequency

Δ (known as population pulsations [24]). In the presence of the spin population relaxation process, the standard OBE predicts a hole burning at $\Delta = 0$ with a linewidth given by the spin relaxation rate $\sim \Gamma_s$ [24]. However, as shown in Figs. 3 and 4, the measured linewidth is orders of magnitude larger than Γ_s (~ 0.1 neV) measured by the phase modulation technique for these QDs [11]. We will establish below that the extra broadening is likely to be due to SD processes involving the spin states.

Similar to the trion SD given in Eq. (2), the effects of spin SD processes on the spin population and coherence are given by,

$$\left. \frac{\partial \rho_{\bar{x},\bar{x}}(\epsilon_t, \epsilon_s)}{\partial t} \right|_{\text{SD}} = \int W_s(\epsilon_t, \epsilon_s; \epsilon'_t, \epsilon'_s) \rho_{\bar{x},\bar{x}}(\epsilon'_t, \epsilon'_s) d\epsilon'_t d\epsilon'_s - \Gamma_s^{SD}(\epsilon_t, \epsilon_s) \rho_{\bar{x},\bar{x}}(\epsilon_t, \epsilon_s) \quad (5)$$

$$\left. \frac{\partial \rho_{x,\bar{x}}(\epsilon_t, \epsilon_s)}{\partial t} \right|_{\text{SD}} = -\Gamma_s^{SD}(\epsilon_t, \epsilon_s) \rho_{x,\bar{x}}(\epsilon_t, \epsilon_s) \quad (6)$$

where the density matrix for each QD in the ensemble is now characterized by two variables, i.e., the zero field trion resonance energy ϵ_t and the spin Zeeman splitting ϵ_s in the external magnetic field plus the local field (e.g., nuclear Overhauser field). Similar to the description of trion SD, W_s is the redistribution kernel and $\Gamma_s^{SD}(\epsilon_t, \epsilon_s) = \int W_s(\epsilon'_t, \epsilon'_s; \epsilon_t, \epsilon_s) d\epsilon'_t d\epsilon'_s$ is the spin SD rate. The qualitative feature of the redistribution kernel function depends critically on the SD mechanism. Local nuclear field fluctuation induced SD only affects the spin Zeeman splitting: $W_s = f(\epsilon_s, \epsilon'_s) \delta(\epsilon_t - \epsilon'_t)$. We note that the inhomogeneous broadening of ϵ_s induced by the nuclear field is given by $\Lambda_s \sim 0.1 \mu\text{eV} \ll \gamma_t$ [28]. We also note that two quantum dots are equally excited if the difference in their resonance frequency for spin to trion transition is much smaller than the trion broadening γ_t . Thus, $\rho_{\bar{x},\bar{x}}(\epsilon_t, \epsilon_s) = \rho_{\bar{x},\bar{x}}(\epsilon'_t, \epsilon'_s)$ if $(\epsilon_t - \epsilon'_t) \pm (\epsilon_s - \epsilon'_s)/2 \ll \gamma_t$. It can then be shown that the two terms on RHS of Eq. (5) cancel each other and hence this mechanism has a negligible effect on the linewidth of the ultra-narrow central spike associated with the spin population pulsation dynamics. On the other hand, if the SD process is due to the interdot transfer of non-equilibrium spin population, it is more reasonable to assume a redistribution kernel $W_s = \Gamma_s^{SD} \exp[-(\epsilon_s - \bar{\epsilon}_s)^2/\Lambda_s^2 - (\epsilon_t - \bar{\epsilon}_t)^2/\Lambda_t^2]/(\pi\Lambda_t\Lambda_s)$ where $\bar{\epsilon}_t$ ($\bar{\epsilon}_s$) is the ensemble averaged trion (spin) resonance energy [21]. In the vicinity of zero detuning $\Delta \ll \gamma_t$, the DT signal is determined by

$$E_{\text{NL}} \simeq \frac{N\sqrt{\pi}|\mu|^4|E_1|^2E_2^*}{8\hbar^3\Lambda_t(2\gamma_t + \Gamma_t^{SD})} \frac{2\Gamma_s + \Gamma_s^{SD}}{\Delta^2 + (2\Gamma_s + \Gamma_s^{SD})^2}. \quad (7)$$

shown as the sharp central spike with linewidth of $2\Gamma_s + \Gamma_s^{SD}$, in Fig. 4 (*Theory*). The experimental data at various magnetic fields are shown in Fig. 4 (*Experiment*), and the measured linewidth of the sharp central spike is plotted in Fig. 5(b) from which we extract $\hbar\Gamma_s^{SD} \sim 0.2 \mu\text{eV}$.

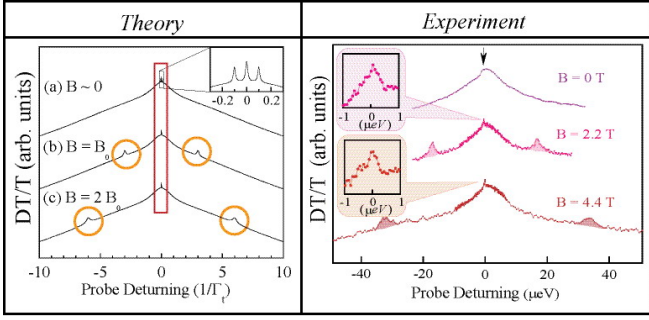


FIG. 4: Comparison of theoretical calculations and experimental results in Voigt geometry. *Theory*: The DT spectrum of 3-level Λ -system at different magnetic field, where $\Lambda_t = 1000\Gamma_t$, $\gamma_t \simeq \Gamma_t/2$, and $\Gamma_s^{SD} = 0.01\Gamma_t$. (a). $B \sim 0$ so that spin inhomogeneous broadening is due to nuclear field $\Lambda_s \sim \Lambda_s^n$. The central spike and the sidebands merge in the limit of vanishing B . (b). $B = B_0$ where $\mu_B \bar{g}_e^x B_0 = 3\hbar\Gamma_t$. Spin inhomogeneous broadening is dominated by the inhomogeneity of the g-factor: $\Lambda_s \simeq \mu_B \Delta g_e^x B/\hbar$. (c). $B = 2B_0$. *Experiment*: SHB lineshapes at different magnetic fields, where the arrow indicates the fixed pump position (1622 meV) and the insets show the zoomed view of central sharp peaks.

In addition to the sharp central spike, the newly emerged SHB features in Voigt geometry also include two symmetric sidebands as highlighted by the ellipse regions in Fig. 3(b). These sidebands can be understood from the perturbation pathway:

$$\rho_{\bar{x},\bar{x}}^{(0)} \xrightarrow{E_1^*} \rho_{\bar{x},\bar{t}}^{(1)} \xrightarrow{E_2} \rho_{\bar{x},x}^{(2)} \xrightarrow{E_1} \rho_{\bar{t},x}^{(3)} \quad (8)$$

associated with stimulated Raman spin excitations [2]. The Stokes and anti-Stokes sidebands appear respectively at $\Delta = \pm\mu_B \bar{g}_e^x B/\hbar$ and their separation as a function of the magnetic field gives the ensemble averaged electron g-factor $\bar{g}_e^x \approx 0.13$ (see Fig. 5(a)), in agreement with earlier reports [2]. As the sideband feature is associated with the Raman spin coherence, it can be inferred from Eq. (6) that spin SD process will broaden the homogeneous linewidth of the sidebands from γ_s to $\gamma_s + \Gamma_s^{SD}$, where γ_s is the spin decoherence rate. The ensemble averaged sideband lineshapes are a convolution of the homogeneous lineshape with the inhomogeneous broadening of the spin Zeeman energy. In the vicinity of $\Delta = \pm\mu_B \bar{g}_e^x B/\hbar$, the nonlinear DT signal is

$$E_{NL} \simeq \frac{N|\mu|^4|E_1|^2 E_2^*(\gamma_s + \Gamma_s^{SD})}{8\hbar^3 \pi \Lambda_t \Lambda_s \gamma_t (\gamma_t + \Gamma_t^{SD})} \times \int \frac{\exp(-(\epsilon_s - \mu_B \bar{g}_e^x B)^2/\Lambda_s^2)}{(\gamma_s + \Gamma_s^{SD})^2 + (|\Delta| - \epsilon_s)^2} d\epsilon_s. \quad (9)$$

At finite magnetic field, the spin inhomogeneous broadening $\Lambda_s(B) = \Lambda_s(0) + \mu_B \Delta g_e^x B$ has the contribution from the inhomogeneity of the electron g-factor Δg_e^x in addition to the nuclear induced zero field inhomogeneous broadening $\Lambda_s(0)$. The sideband linewidth measured at

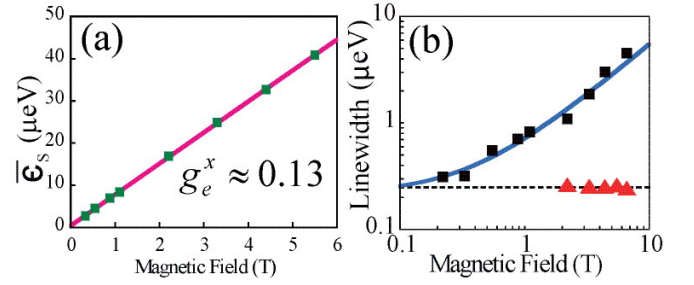


FIG. 5: (a). The separation between Stokes and anti-Stokes sidebands is plotted as a function of magnetic field, and the linear fitting gives the ensemble averaged electron in-plane g-factor $|\bar{g}_e^x| = 0.13$. (b). The linewidth extracted from the experimental data at various magnetic fields, where \blacksquare (\blacktriangle) are the SHB linewidth of the sidebands (central sharp spike), highlighted in Fig. 3(b) with ellipse (square) region. The solid curve is the calculated sidebands linewidth based on Eq. (9) (see text). The dashed line is a guide to the eye.

various magnetic fields is shown in Fig. 5(b), which is consistent with that calculated using Eq. (9) with parameters as $\hbar(\gamma_s + \Gamma_s^{SD}) \simeq 0.18 \mu\text{eV}$ and $\Lambda_s \simeq 0.64B \mu\text{eV/T} + 0.1 \mu\text{eV}$. As $\gamma_s \ll \Gamma_s^{SD}$ from the theoretical investigation of both the nuclear and phonon induced spin decoherence [12, 13], we can get $\hbar\Gamma_s^{SD} = 0.18\mu\text{eV}$ which agrees with the value of Γ_s^{SD} extracted from the central narrow spike. In addition, the spin g-factor variation Δg_e^x is determined to be 0.01 from Λ_s , so $\Delta g_e^x/\bar{g}_e^x \simeq 0.1$, in agreement with transient spin quantum beat measurements [2].

In summary, we have shown in this paper that SD from the trion state complicates the trion SHB profile, and makes an important contribution to the double-Lorentzian-like lineshape. In the Voigt geometry, we have found a complex lineshape arising from spin dynamics in the spectral hole burning: a narrow central spike and two symmetric Stokes and anti-Stokes sidebands. They have been theoretically identified to result as consequence of spin population pulsation dynamics and stimulated Raman spin coherence, respectively. Moreover, a spin SD process is observed in contributions to the SHB lineshape, and has been theoretically identified as interdot transfer of the non-equilibrium spin population. Possible mechanisms include the interdot spin flip-flop interactions of the electrons or spin conserved electron tunneling to adjacent neutral dots. Their quantitative estimates can not be determined without a detailed calculation which is beyond the scope of the paper. Nevertheless, the existence of these decoherence mechanisms revealed by our experiments will have important impacts on the efforts towards spin based quantum applications in these kinds of QDs.

This work was supported in part by the U.S. ARO, NSA/LPS, ARDA, AFOSR, ONR, and FOCUS-NSF.

* Present Address: Department of Biomedical Engineering, University of Michigan, Ann Arbor, MI 48109

† Present Address: Department of Physics, The University of Texas, Austin, TX 78712

‡ Electronic address: dst@umich.edu

- [1] D. D. Awschalom, D. Loss, and N. Samarth, *Semiconductor Spintronics and Quantum Computing* (Springer, New York, 2002).
- [2] M. V. G. Dutt, J. Cheng, B. Li, X. Xu, X. Li, P. R. Berman, D. G. Steel, A. S. Bracker, D. Gammon, S. E. Economou, et al., Phys. Rev. Lett. **94**, 227403 (2005).
- [3] J. R. Petta, A. C. Johnson, J. M. Taylor, E. A. Laird, A. Yacoby, M. D. Lukin, C. M. Marcus, M. P. Hanson, and A. C. Gossard, Science **309**, 2180 (2005).
- [4] F. H. L. Koppens, C. Buizert, K. J. Tielrooij, I. T. Vink, K. C. Nowack, T. Meunier, L. P. Kouwenhoven, and L. M. K. Vandersypen, Nature **442**, 766 (2006).
- [5] T. Fujisawa, D. G. Austing, Y. Tokura, Y. Hirayama, and S. Tarucha, Nature **419**, 278 (2002).
- [6] R. Hanson, B. Witkamp, L. M. K. Vandersypen, L. H. W. van Beveren, J. M. Elzerman, and L. P. Kouwenhoven, Phys. Rev. Lett. **91**, 196802 (2003).
- [7] J. M. Elzerman, R. Hanson, L. H. W. van Beveren, B. Witkamp, L. M. K. Vandersypen, and L. P. Kouwenhoven, Nature **430**, 431 (2004).
- [8] M. Kroutvar, Y. Ducommun, D. Heiss, M. Bichler, D. Schuh, G. Abstreiter, and J. J. Finley, Nature **432**, 81 (2004).
- [9] A. V. Khaetskii and Y. V. Nazarov, Phys. Rev. B **64**, 125316 (2001).
- [10] I. A. Merkulov, A. L. Efros, and M. Rosen, Phys. Rev. B **65**, 205309 (2002).
- [11] J. Cheng, Y. Wu, X. Xu, D. Sun, D. G. Steel, A. S. Bracker, D. Gammon, W. Yao, and L. J. Sham, Solid State Communications **140**, 381 (2006).
- [12] V. N. Golovach, A. Khaetskii, and D. Loss, Phys. Rev. Lett. **93**, 016601 (2004).
- [13] W. Yao, R.-B. Liu, and L. J. Sham, Phys. Rev. B **74**, 195301 (2006).
- [14] R. de Sousa and S. Das Sarma, Phys. Rev. B **67**, 033301 (2003).
- [15] J. G. Tischler, A. S. Bracker, D. Gammon, and D. Park, Phys. Rev. B **66**, 081310 (2002).
- [16] P. R. Berman and R. G. Brewer, Phys. Rev. A **32**, 2784 (1985).
- [17] P. Meystre and M. S. III, *Elements of Quantum Optics* (Springer, Berlin, 1998).
- [18] H. Wang, M. Jiang, and D. G. Steel, Phys. Rev. Lett. **65**, 1255 (1990).
- [19] H. Wang and D. G. Steel, Phys. Rev. A **43**, 3823 (1991).
- [20] N. H. Bonadeo, G. Chen, D. Gammon, D. S. Katzer, D. Park, and D. G. Steel, Phys. Rev. Lett. **81**, 2759 (1998).
- [21] We have assumed the strong redistribution model for interdot trion and spin spectral diffusion where the kernel only depends on the final state density [16].
- [22] B. D. Fried and S. D. Conte, *The Plasma Dispersion Function* (Academic Press, New York, 1961).
- [23] M. V. G. Dutt, J. Cheng, D. G. Steel, A. S. Bracker, D. Gammon, and L. J. Sham, Solid State Communications **140**, 374 (2006).
- [24] D. G. Steel and S. C. Rand, Phys. Rev. Lett. **55**, 2285 (1985).
- [25] J. G. Tischler, A. S. Bracker, D. Gammon, and D. Park, Phys. Rev. B **66**, 081310 (2002).
- [26] M. Atatüre, J. Dreiser, A. Badolato, A. Högele, K. Karrai, and A. Imamoglu, Science **312**, 551 (2006).
- [27] X. Xu, Y. Wu, B. Sun, Q. Huang, J. Cheng, D. G. Steel, A. S. Bracker, D. Gammon, C. Emary, and L. J. Sham, Phys. Rev. Lett. **99**, 097401 (2007).
- [28] A. S. Bracker, E. A. Stinaff, D. Gammon, M. E. Ware, J. G. Tischler, A. Shabaev, A. L. Efros, D. Park, D. Gershoni, V. L. Korenev, et al., Phys. Rev. Lett. **94**, 047402 (2005).